

Intersubband Emission from Semiconductor Superlattices Excited by Sequential Resonant Tunneling

M. Helm, P. England, E. Colas, F. DeRosa, and S. J. Allen, Jr.

Bellcore, Red Bank, New Jersey 07701-7040

(Received 30 March 1989)

We present the first observation of infrared light emission from a semiconductor superlattice in a resonant-tunneling experiment. Radiation from the three lowest intersubband transitions is observed, proving resonant tunneling an effective means of populating high-lying states of the superlattice. The relative strength of the emission lines enables us to estimate the electron temperature below the optical-phonon energy to reach about 140 K, whereas transitions originating above the optical-phonon energy are strongly quenched.

PACS numbers: 73.40.Gk, 78.60.-b, 78.65.Fa

Soon after the first proposal by Esaki and Tsu¹ of semiconductor superlattices, the problem of generating and amplifying infrared light in these systems was theoretically addressed by Kazarinov and Suris.² There they suggested that photon-assisted tunneling could lead to gain or infrared emission. However, direct optical transitions between energy levels in superlattices or quantum wells (subbands or minibands) also appear attractive for the generation of infrared radiation due to the large electric dipole moment between them.³ Indeed, several schemes to achieve a population inversion and lasing action between subbands or minibands have been proposed.^{4,5} To achieve this goal it is clear that experiments must go beyond the simple Ohmic heating of quantum confined systems that has been used in the past,^{6,7} since this technique does not appear to have the potential for producing gain. In this Letter we report the first observation of intersubband emission from a superlattice excited by sequential resonant tunneling. Electrons are injected into an excited bound state of the first quantum well, where they relax by emitting phonons and photons, and subsequently tunnel into an excited state of the adjacent well. This process is repeated throughout the whole superlattice. We observe radiation stemming from the three lowest intersubband transitions. This is the first experiment which uses tunneling to create hot carriers capable of emitting radiation and establishes a fundamental step towards the realization of an intersubband laser.

The GaAs/Al_{0.3}Ga_{0.7}As superlattice was grown by organometallic chemical vapor deposition on an n^+ substrate and consists of 60 periods of 350-Å-wide GaAs wells and 100-Å-thick AlGaAs barriers. The superlattice was not intentionally doped, resulting in an n -type background of $n \approx 5 \times 10^{15} \text{ cm}^{-3}$, and is sandwiched between n^+ GaAs buffer and cap layers, both of thickness 0.5 μm .

In the following we will discuss some of the issues involved in the design of a resonant-tunneling superlattice radiator. The quantum efficiency, η , for light emission in

semiconductors is given by the ratio of the radiative relaxation rate, W_r , to the total relaxation rate between two levels,⁸ that is, $\eta = W_r / (W_r + W_{nr})$, where W_{nr} is the nonradiative relaxation rate. For electrons within the conduction band of a semiconductor superlattice this ratio is usually very small, since optical-phonon emission occurs on a picosecond time scale⁹ whereas typical radiative processes between quantum well levels are of the order of microseconds. However, as long as electrons are not capable of emitting optical phonons, their nonradiative relaxation rate is reduced by about 2 orders of magnitude to $10^9 - 10^{10} \text{ s}^{-1}$, limited by acoustic-phonon emission,¹⁰ thus improving the quantum efficiency. In the present superlattice the energies of the first five subbands, calculated according to Bastard's model,¹¹ are $E_1 = 3.8 \text{ meV}$, $E_2 = 15.2 \text{ meV}$, $E_3 = 34.1 \text{ meV}$, $E_4 = 60.5 \text{ meV}$, and $E_5 = 94.2 \text{ meV}$. Because of the thick barriers, the levels are localized states rather than extended minibands. Three subbands lie below the optical-phonon energy of $\hbar\omega_{op} = 36 \text{ meV}$ for GaAs.

It is well known that transitions between subbands in quantum wells are allowed only for light polarized perpendicular to the layers.¹² This poses an experimental difficulty for both absorption and emission measurements. In the latter case, the emitted radiation leaves the sample mainly at the edges, leading to undetectably small signals (at least as long as there is absorption rather than gain in the medium). Recently we have shown that it is possible to overcome this problem by depositing a metallic grating on the surface of the sample, which essentially converts the radiation propagating along the layers into a wave radiating from the surface.⁷ This method was also employed in the present experiment. Gratings with periods between 8 and 30 μm were defined photolithographically (area $3 \times 4 \text{ mm}^2$), after which Sn (150 Å) and Au (1500 Å) were evaporated. After lift-off, the grating was alloyed at 400°C to serve as the top electrical contact. Then, by using the grating as an etch mask, the highly absorbing top n^+ GaAs layer was etched away between the metal stripes. Finally, the

second contact was made by alloying In at the bottom of the sample. In order to study in detail the current-voltage characteristics of the structure we also fabricated mesas with 200- μm diameter (about 500 times smaller area than the grating structure).

Figure 1 shows the current-voltage characteristics of a mesa structure at 10 K. Many extremely sharp negative differential resistances (NDR's) are observed, similar to those reported in the initial work of Esaki and Chang,¹³ and later by Choi *et al.*¹⁴ and Vuong, Tsui, and Tsang.¹⁵ The origin of these NDR's is sequential resonant tunneling in connection with a high-electric-field domain expanding through the superlattice. Each single NDR region corresponds to a single superlattice period breaking off from a resonant condition (i.e., ground state in resonance with an excited state in the adjacent well), and aligning to resonance with the next higher level (see inset of Fig. 1).^{14,15} The most pronounced NDR's occur whenever the superlattice breaks off from being homogeneously aligned. This enables us to identify the energy levels between which tunneling takes place (numbers in Fig. 1). Consequently, we can determine the energy level into which the electrons are injected at a certain voltage. The energy levels deduced from the current-voltage characteristics are in reasonable agreement with the calculated ones. The main features of Fig. 1 could also be observed with the grating structure, although not as clearly. The current density in these structures is basically determined by the barrier thicknesses. The thickness of 100 Å, chosen in the present experiment, leads to a current of a few tens of mA in the grating structure when injecting into the fourth or fifth subband. This results in sufficient electrical power to expect an observable

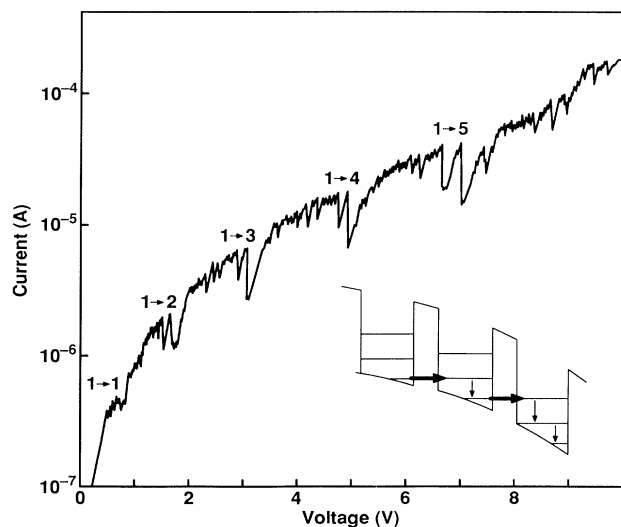


FIG. 1. Current-voltage characteristic of the superlattice (mesa with 200- μm diam) at 4.2 K. The numbers indicate the relevant tunneling processes. Inset: Schematic of conduction-band edge together with transport and relaxation paths.

emission signal without overheating the sample.

The experimental setup for studying emission from the superlattices was as follows: Voltage pulses of several ms duration were applied to the sample, which was kept at a temperature of 10 to 20 K. The resulting radiation was guided with a light pipe to a high-sensitivity Si bolometer operated at 1.5 K. In order to analyze the spectrum of the emitted radiation, a tunable absorber consisting of a wedged slab of InSb ($n \approx 10^{14} \text{ cm}^{-3}$) was placed between the superlattice and the bolometer in the center of a superconducting magnet. By application of a magnetic field the cyclotron resonance absorption frequency in the InSb was varied, providing a tunable filter.⁷ The filter was calibrated with a Fourier-transform spectrometer. The spectral resolution was about 20 cm^{-1} (2.5 meV or 0.3 T); the rejection was 50% for unpolarized light. Because of the small effective mass of InSb a magnetic field sweep from 0 to 6 T corresponds to a frequency scan from 0 to 325 cm^{-1} (40-meV photon energy). As a consequence of this detection technique, minima in the detected signal will be observed at magnetic field values where the InSb cyclotron resonance frequency coincides with the frequency of the emitted radiation.

Figure 2 shows the emission signal as a function of the InSb magnetic field. The two top curves are for a sample with a 12- μm -period grating, biased at 8 (curve *a*) and 9 V (curve *b*); the lower trace represents the emis-

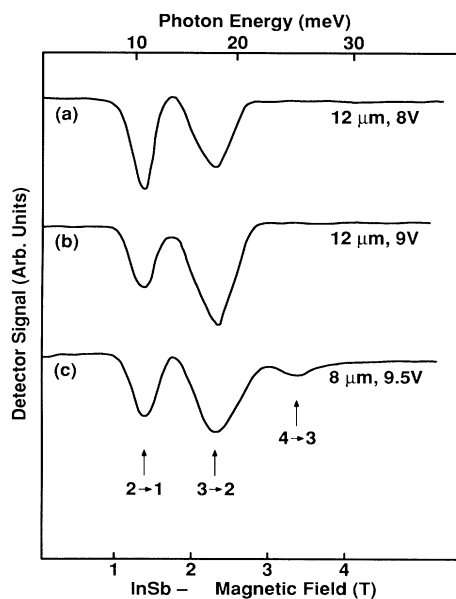


FIG. 2. Detector signal vs magnetic field of InSb filter and corresponding photon energy for samples with different grating periods at bias voltages as indicated. The observed intersubband transitions are marked. The peak absorption is about 20%; the magnitude of the signal in curve *b* has been reduced by a factor of 2.5.

sion from a sample with an 8- μm -period grating at 9.5 V (curve *c*). The absorptive features occur at magnetic field values of 1.35, 2.35, and 3.4 T, corresponding to photon energies of 11, 18, and 25 meV, respectively. In comparison, the calculated transition energies (without electric field) between the four lowest subbands, E_{12} , E_{23} , and E_{34} , are 11.4, 18.9, and 26.4 meV. From this agreement we conclude that we are observing intersubband light emission. With the 12- μm sample, the relative strength of the 3-2 transition increases with respect to the 2-1 transition upon increasing the voltage from 8 to 9 V. The current rises thereby from 35 to 75 mA (nearly exponentially, as expected for a tunneling process) and the emission intensity increases by a factor of 3, that is, faster than the electrical input power. Below 6 V no emission signal could be detected, because the current and the input power become too small. As a result, emission can only be analyzed over a small part of the I - V curve. In curve *c* we note that the 8- μm grating enables us to observe weak radiation from the 4-3 subband transition. These results show that sequential resonant tunneling is much more effective than Ohmic heating,⁷ since electrons are injected directly into high-lying states. The conversion efficiency of electrical input power into intersubband radiation power is at least 1 order of magnitude better in the present case.

It is striking that the observed transition energies appear hardly affected by the strong electric field across the superlattice and agree so well with the flat-quantum-well calculation. This suggests that most of the voltage drops across the barriers rather than the wells. The screening of the electric field in the well can arise from electron accumulation on the positive side of each well and hole accumulation on the negative side. Since there are no holes before bias is applied, they are created through impact ionization, initiated by electrons accelerated up to energies of several eV. We found strong support for this assumption by observing GaAs-band-gap luminescence from the biased superlattice.

The relative strengths of the emission lines can be used to determine the effective electron temperature provided the relative grating coupler efficiency is known. In order to better understand the coupling mechanism of the grating to the intersubband transition, we performed grating-coupled absorption measurements in similar superlattices grown on a semi-insulating substrate. The measurements were performed with a Fourier-transform spectrometer at fixed temperatures between 50 and 130 K. For a certain intersubband transition to be observed, the period of the grating must be smaller than the wavelength corresponding to the respective transition, λ , divided by the refractive index of the material ($n_r = 3.5$ for GaAs). The coupling is strongest when λ/n_r is close to the grating period and decreases slowly towards longer wavelengths. Emission measurements on samples with 30-, 22-, and 16- μm periods also revealed intersubband

transitions; the line shape, however, seemed distorted by the vicinity of the grating resonance. This consideration can possibly explain the fact that the 4-3 transition can be observed with the 8- μm grating, but not with the 12- μm grating.

In Fig. 3 the conduction-band edge of the superlattice at a bias voltage of approximately 8 V is sketched. At this bias, according to the current-voltage characteristics (Fig. 1), electrons are injected into the fifth electric subband. From there they relax into the ground state by emitting photons and mainly phonons, or leak out through the barrier without relaxing, giving rise to impact ionization after they have gained enough energy. The energy of the LO phonons in GaAs is indicated by the dashed line. It becomes clear now why the two lower transitions can be observed so clearly, whereas the two upper transitions remain very weak or undetectable. While the estimated radiative relaxation rate for the 4-3 transition is at most 3 times larger than for the 3-2 transition ($W_r \propto \omega^2 f$, where ω is the transition frequency and f the oscillator strength), the nonradiative rate increases by 2 orders of magnitude, because the channel for optical-phonon emission is available. This drastically reduces the quantum efficiency and, hence, the magnitude of the 4-3 emission signal.

We now use the relative strengths of the two transitions in trace *b* of Fig. 2 to determine the effective temperature of the electron system, or instead, if a population inversion exists. To answer this question, we have to consider the factors determining the emitted line strengths. The power emitted in each line is given by

$$P = \hbar \omega W_r n C V, \quad (1)$$

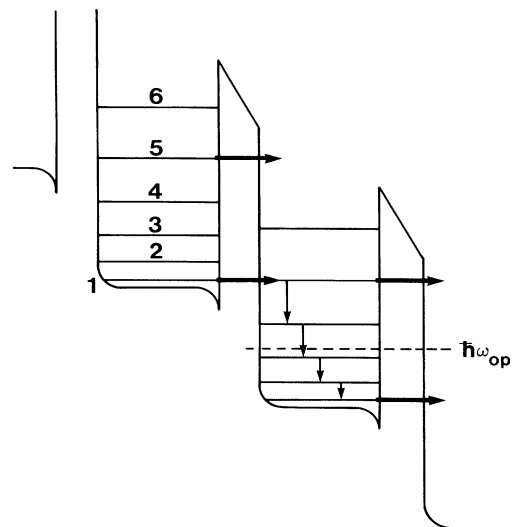


FIG. 3. Schematic of the conduction band of the superlattice at a bias of about 8 V. The tunneling and relaxation processes are indicated, as well as the optical-phonon energy.

where W_r is the spontaneous emission rate, n is the electron density in the excited level, V is the volume of the sample, and C is a coupling constant, describing the efficiency with which radiation generated in a certain transition eventually leaves the sample. C obviously includes the influence of the grating. Knowing the ratios of P , W_r , and C for the different transitions, it is possible to determine the respective electron population ratio. The relative grating coupling strength has been determined by the absorption measurement described above, and is about 1.2 ± 0.2 times larger for the higher transition. The power ratio is simply measured from the area under the lines in Fig. 2, and the emission rates are evaluated by noting that the oscillator strength for the 3-2 transition is about twice as large as for the 2-1 transition³ (neglecting the electric field). From this, the population ratio n_3/n_2 is calculated to be 0.23 ± 0.05 , corresponding to an intersubband temperature of 140 ± 20 K. Above the optical-phonon energy, the electrons are cooled more effectively and the temperature is much lower. As an illustration consider a temperature of 120 K and assume the grating coupling to be the same for all transitions. Then, according to Eq. (1), the ratio of the emitted power in each line, $P_{21}:P_{32}:P_{43}$, would equal 9:14:5, so the 4-3 transition would be about half as strong as the 2-1 transition. In the experiment, however, the 4-3 transition is barely visible (curve *c* in Fig. 2). Thus we conclude that the electron distribution is not inverted, being very hot below the optical-phonon energy, but significantly cooler above the optical-phonon energy.

In conclusion, we have demonstrated emission of infrared light from a superlattice excited by sequential resonant tunneling, realizing an idea that has been incubating as long as the concept of the superlattice itself. This method of excitation has the potential for directly pump-

ing, by electrical means, excited states of the quantum well, and the potential for producing population inversion. We look forward to experiments and theoretical modeling to ascertain whether these conditions can be achieved.

¹L. Esaki and R. Tsu, IBM J. Res. Dev. **14**, 61 (1970).

²R. F. Kazarinov and R. A. Suris, Fiz. Tekh. Poluprovodn. **5**, 797 (1971) [Sov. Phys. Semicond. **5**, 707 (1971)]; **6**, 148 (1972) [**6**, 120 (1972)].

³L. C. West and S. J. Eglash, Appl. Phys. Lett. **46**, 1156 (1985).

⁴F. Capasso, K. Mohammed, and A. Y. Cho, IEEE J. Quantum Electron. **22**, 1853 (1986).

⁵P.-F. Yuh and K. L. Wang, Appl. Phys. Lett. **51**, 1404 (1987); K. L. Wang and P.-F. Yuh, IEEE J. Quantum Electron. **25**, 12 (1989).

⁶E. Gronik, R. Schawarz, D. C. Tsui, A. C. Gossard, and W. Wiegmann, Solid State Commun. **38**, 541 (1981).

⁷M. Helm, E. Colas, P. England, F. DeRosa, and S. J. Allen, Jr., Appl. Phys. Lett. **53**, 1714 (1988).

⁸E. Gronik, in *Narrow Gap Semiconductors. Physics and Applications*, edited by W. Zawadzki, Lecture Notes in Physics Vol. 133 (Springer-Verlag, Berlin, 1980), p. 160.

⁹A. Seilmeier, H. J. Hübner, G. Abstreiter, G. Weimann, and W. Schlapp, Phys. Rev. Lett. **59**, 1345 (1987).

¹⁰D. Y. Oberli, D. R. Wake, M. V. Klein, J. Klem, T. Henderson, and H. Morkoc, Phys. Rev. Lett. **59**, 696 (1987).

¹¹G. Bastard, Phys. Rev. B **24**, 5693 (1981).

¹²F. Stern, Phys. Rev. Lett. **33**, 960 (1974).

¹³L. Esaki and L. L. Chang, Phys. Rev. Lett. **33**, 495 (1974).

¹⁴K. K. Choi, B. F. Levine, R. J. Malik, J. Walker, and C. G. Bethea, Phys. Rev. B **35**, 4172 (1987).

¹⁵T. H. H. Vuong, D. C. Tsui, and W. T. Tsang, Appl. Phys. Lett. **52**, 981 (1988).